Phonons and superconductivity in fcc and dhcp lanthanum

S. Bağcı,[1] H. M. Tütüncü,[1] S. Duman,[1] and G. P. Srivastava[2]
[1]*Sakarya Üniversitesi, Fen-Edebiyat Fakültesi, Fizik Bölümü, 54187 Adapazarı, Turkey*
[2]*School of Physics, University of Exeter, Stocker Road, Exeter EX4 4QL, United Kingdom*
(Received 4 January 2010; revised manuscript received 25 March 2010; published 19 April 2010)

We have investigated the structural and electronic properties of lanthanum in the face-centered-cubic (fcc) and double hexagonal-close-packed (dhcp) phases using a generalized gradient approximation of the density functional theory and the *ab initio* pseudopotential method. It is found that double hexagonal-close-packed is the more stable phase for lanthanum. Differences in the density of states at the Fermi level between these two phases are pointed out and discussed in detail. Using the calculated lattice constant and electronic band structure for both phases, a linear response approach based on the density functional theory has been applied to study phonon modes, polarization characteristics of phonon modes, and electron-phonon interaction. Our phonon results show a softening behavior of the transverse acoustic branch along the Γ-L direction and the Γ-M direction for face-centered-cubic and double hexagonal-close-packed phases, respectively. Thus, the transverse-phonon linewidth shows a maximum at the zone boundary $M(L)$ for the double hexagonal-close-packed phase (face-centered-cubic phase), where the transverse-phonon branch exhibits a dip. The electron-phonon coupling parameter λ is found to be 0.97 (1.06) for the double hexagonal-close-packed phase (face-centered-cubic phase), and the superconducting critical temperature is estimated to be 4.87 (dhcp) and 5.88 K (fcc), in good agreement with experimental values of around 5.0 (dhcp) and 6.0 K (fcc). A few superconducting parameters for the double hexagonal-close-packed phase have been calculated and compared with available theoretical and experimental results. Furthermore, the calculated superconducting parameters for both phases are compared between each other in detail.

DOI: 10.1103/PhysRevB.81.144507 PACS number(s): 74.25.Kc, 71.15.Mb, 74.25.Jb, 71.20.Eh

I. INTRODUCTION

The unique physical and chemical properties of the rare-earth metals have attracted interest for decades. Lanthanum (La), the first member of the rare-earth series of elements, can exist in both the double hexagonal-close-packed (dhcp) phase and the face-centered-cubic (fcc) phase. Naturally formed La includes both crystalline phases. This metal has particularly interesting properties and has widespread use in the metallurgy industry. Due to high electronic density of states at the Fermi surface and specific phonon spectrum, one would expect strong electron phonon coupling, and therefore a reasonable high superconducting transition temperature, for La. This has led to several experimental studies[1–12] on the superconducting properties of lanthanum. These studies showed that both phases of La are superconducting, with the superconducting transition temperature near 5 K for dhcp and near 6 K for fcc. These experimental works have provided impetus for theoretical studies of this material. These include the self-consistent linear-muffin-tin-orbital (LMTO) method,[13–17] non-self-consistent relativistic augment plane wave (RAPW) method,[18] full potential linearized augmented plane wave method (LAPW),[19–21] and the well-known Ashcrofts's empty core (EMC) model.[22] An anomalous phonon spectrum of fcc La has been measured by using coherent inelastic neutron-scattering techniques.[23] On the theoretical side, considerable progress has been made in the description of the vibrational properties of fcc La. An eight nearest-neighbor force-constant model[23] and a linear response method based on the density functional perturbation theory[24,25] have been used to calculate the phonon spectrum and density of states for the fcc La.

Although considerable progress has been made in theoretical[23–25] and experimental[23] description of the vibrational properties of the fcc La, no experimental and theoretical results are available for the phonon spectrum and density of states of dhcp La. It is important to thoroughly study the static, electronic and vibrational properties of both phases of this material. In this work, we have employed the *ab initio* pseudopotential method and the density functional theory within a generalized gradient approximation to obtain structural properties of lanthanum in the face-centered-cubic and double hexagonal-close-packed phases and to provide a comparison with calculations and experimental data available in the literature. We have further carried out *ab initio* linear response calculations of the lattice dynamics, electron-phonon interaction, and a discussion on the polarization characteristics of zone-center phonon modes. The electron-phonon mass enhancement parameter λ is used to obtain the superconducting parameters and compared with previous theoretical and experimental results. Finally, the superconducting parameters for the fcc La and dhcp are compared with each other and an explanation is provided for any differences.

II. THEORY

The present investigation is carried out by using the code PWSCF.[26] It employs a plane-wave basis set for the expansion of the Kohn-Sham orbitals. The wave functions is expanded in plane waves with the energy cutoff of 60 Ry and the electronic charge density is expanded in a basis cut off up to 400 Ry. The Kohn-Sham equations[27] were solved using an iterative conjugate gradient scheme to obtain total energy.

The Vanderbilt ultrasoft pseudopotential[28] for the description of the electron-ion interaction was used. We have to mention that the $4f$ shell of lanthanum atom is not included in our pseudopotential either as core or as valence. The reason for this is that superconducting tunneling experiments[5,8] on La showed that this element is d-type superconductor, with electron-phonon coupling constant around 0.8–0.9. On the theoretical side, previous band structure investigations[19,20] for La indicated that the $4f$ electronic states lie a few electron volts above the Fermi level even up to $P=120$ kbar and do not play a direct role in determining the physical properties and phonon spectrum of this material. We have provided a good test of this ultrasoft pseudopotential in our previous paper,[25] where it was pointed out that the calculated results for ground-state and vibrational properties of fcc La are in good agreement with previous experimental and theoretical results. Thus, we are safe to use this pseudopotential for dhcp La as well. The density functional theory has been implemented within a generalized gradient approximation (GGA), using the Perdew-Burke-Ernzerhof method.[29] Self-consistent solutions of the Kohn-Sham equations were obtained by employing a set of Monkhorst-Pack special $\mathbf{k}$ points[30] within the irreducible part of the Brillouin zone (IBZ). Since both crystal structures considered here are metallic, convergence is reached using 145 (270) $\mathbf{k}$ points in the IBZ of the fcc (dhcp) structure. The electronic charge density and the electronic density of states were calculated with $(32\times32\times32)$ and $(28\times28\times28)$ Monkhorst-Pack $\mathbf{k}$-point meshes for fcc and dhcp La, respectively.

We used $(16\times16\times16)$ and $(14\times14\times14)$ $\mathbf{k}$-points grids for the sampling the IBZ for phonon calculations in fcc and dhcp La, respectively. The phonon frequencies and atomic displacements were subsequently obtained using the linear response method,[26,31] which avoids the use of supercells and allows the calculation of the dynamical matrix at arbitrary $\mathbf{q}$ vectors. The eigenfrequencies and eigenvectors of lattice vibrations are calculated within the framework of self-consistent density functional perturbation theory (DFPT).[26,31] A static linear response of the valence electrons was considered in terms of the variation in the external potential corresponding to periodic displacements of the atoms in the unit cell. The screening of the electronic system in response to the displacement of the atoms was taken into account in a self-consistent manner. In order to obtain full phonon spectrum, we evaluated 29 dynamical matrices on a $(8\times8\times8)$ grid in $\mathbf{q}$ for the fcc La, and 24 matrices (on $(4\times4\times4)$ grid) for the dhcp La. These dynamical matrices were Fourier transformed to obtain the full phonon spectrum and density of states. We estimate that the phonon frequencies are accurate to within 0.1 THz for the present choice of the kinetic energy cutoff and the special $\mathbf{k}$ points.

The electron-phonon spectral function $\alpha^2F(\omega)$ can be written as[32–34]

$$\alpha^2F(\omega)=\frac{1}{2\pi N(E_F)}\sum_{\mathbf{q}j}\frac{\gamma_{\mathbf{q}j}}{\hbar\omega_{\mathbf{q}j}}\delta(\omega-\omega_{\mathbf{q}j}), \tag{1}$$

where $N(E_F)$ is the electronic density of states per atom and spin at the Fermi level and $\gamma_{\mathbf{q}j}$ is the phonon linewidth. When the electron energies around the Fermi level are linear in the range of phonon energies, the phonon linewidth is given by the Fermi's "golden rule" formula[33,34]

$$\gamma_{\mathbf{q}j}=2\pi\omega_{\mathbf{q}j}\sum_{\mathbf{k}nm}|g^{\mathbf{q}j}_{(\mathbf{k}+\mathbf{q})m;\mathbf{k}n}|^2\delta(\varepsilon_{\mathbf{k}n}-\varepsilon_F)\delta(\varepsilon_{(\mathbf{k}+\mathbf{q})m}-\varepsilon_F), \tag{2}$$

where the Dirac delta functions express energy conservation conditions. The matrix element for electron-phonon interaction is[33,34]

$$g^{\mathbf{q}j}_{(\mathbf{k}+\mathbf{q}),m;\mathbf{k}n}=\sqrt{\frac{\hbar}{2M\omega_{\mathbf{q}j}}}\langle\phi_{(\mathbf{k}+\mathbf{q})m}|\mathbf{e}_{\mathbf{q}j}\cdot\vec{\nabla}V^{\mathrm{SCF}}(\mathbf{q})|\phi_{\mathbf{k}n}\rangle, \tag{3}$$

where M is atomic mass and $\vec{\nabla}V^{\mathrm{SCF}}(\mathbf{q})$ is the derivative of the self-consistent effective potential with respect to the atomic displacement caused by a phonon with wave vector $\mathbf{q}$.

The electron-phonon coupling parameter involving a phonon $\mathbf{q}j$ can be expressed as[33,34]

$$\lambda_{\mathbf{q}j}=\frac{\gamma_{\mathbf{q}j}}{\pi\hbar N(\varepsilon_F)\omega^2_{\mathbf{q}j}}. \tag{4}$$

The electron-phonon mass enhancement parameter λ is a good measure of the overall strength of the electron-phonon interaction; it is given as

$$\lambda=\sum_{qj}\lambda_{qj}W(\mathbf{q}), \tag{5}$$

where $W(\mathbf{q})$ is the weight of the $\mathbf{q}^{\mathrm{th}}$ special phonon wave vector. From λ, several properties related to superconductivity can be obtained. According to McMillian,[32] one can write the electron-phonon mass enhancement parameter as

$$\lambda=\frac{\eta}{M\langle\omega^2\rangle}. \tag{6}$$

Here, η is the Hopfield parameter (electronic stiffness constant) and $\langle\omega^2\rangle$ second moment of phonon spectrum. In general, $\langle\omega^n\rangle$ can be given as[32–34]

$$\langle\omega^n\rangle=\frac{1}{\lambda}\sum_{\mathbf{q}j}\lambda_{\mathbf{q}j}\omega^n_{\mathbf{q}j}. \tag{7}$$

The electronic heat-capacity coefficient γ_{ehc} is proportional to electronic density of states at the Fermi level times the enhancement factor $(1+\lambda)$. After calculating λ and $N(E_F)$, γ_{ehc} can be obtained from

$$\gamma_{\mathrm{ehc}}=\frac{2}{3}\pi^2k_B^2N(E_F)(1+\lambda). \tag{8}$$

The superconducting transition temperature T_C was estimated on the basis of the Allen-Dynes modification of the McMillian formula[33,34]

$$T_C=\frac{\omega_{\ln}}{1.2}\exp\left(-\frac{1.04(1+\lambda)}{\lambda-\mu^*(1+0.62\lambda)}\right), \tag{9}$$

where μ^* is a Coulomb pseudopotential and $\omega_{\ln}$ is the logarithmically averaged frequency

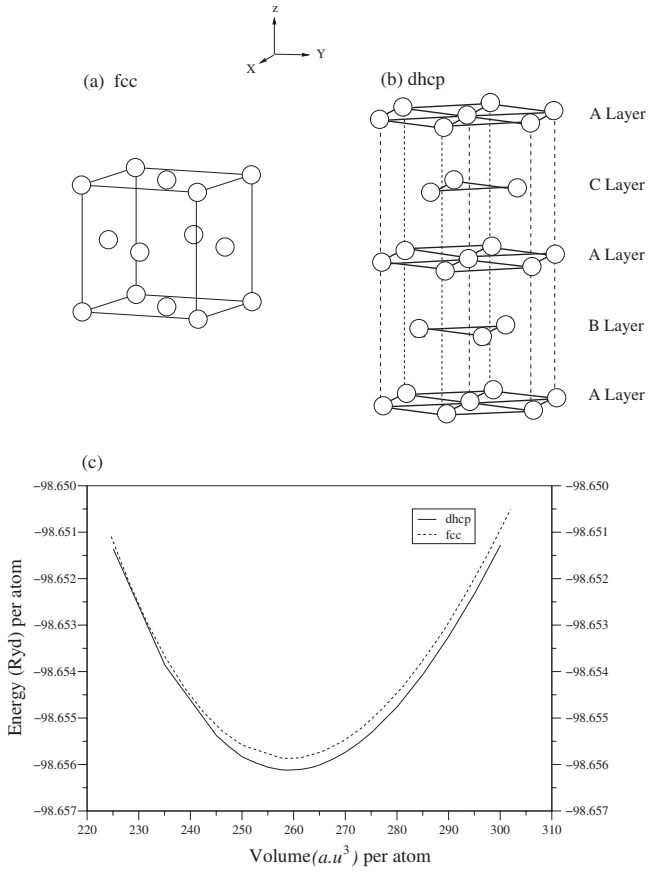

FIG. 1. (a) The face-centered-cubic structure (fcc) of lanthanum. (b) The double hexagonal-close-packed (dhcp) structure of lanthanum. The layers of atoms are also indicated. (c) Calculated total energies as a function of volume for both phases of lanthanum.

$$\omega_{\ln} = \exp\left(\frac{1}{\lambda}\sum_{\mathbf{q}j} \lambda_{\mathbf{q}j} \ln \omega_{\mathbf{q}j}\right). \tag{10}$$

In our calculations, the Coulomb pseudopotential μ^* is assumed to be 0.12. T_C leads us to calculate the value of the attractive interaction between electron pair in the superconductor (V_p). The formula for V_p is written as[32–34]

$$N(E_F)V_p = \left(\ln\left(\frac{1.14\Theta_D}{T_C}\right)\right)^{-1}. \tag{11}$$

Using the value of T_C, one can calculate the gap energy (2Δ), which is needed to break up a Cooper pair,

$$2\Delta = 3.53 k_B T_C. \tag{12}$$

The summations in Eqs. (1) and (2) are performed using a dense mesh [$(28\times28\times28)$ Monkhorst-Pack mesh] of **k** points in the irreducible Brillouin zone of the both structures. The Dirac delta functions in this equation were replaced with a Gaussian function of width 0.020 Ry.

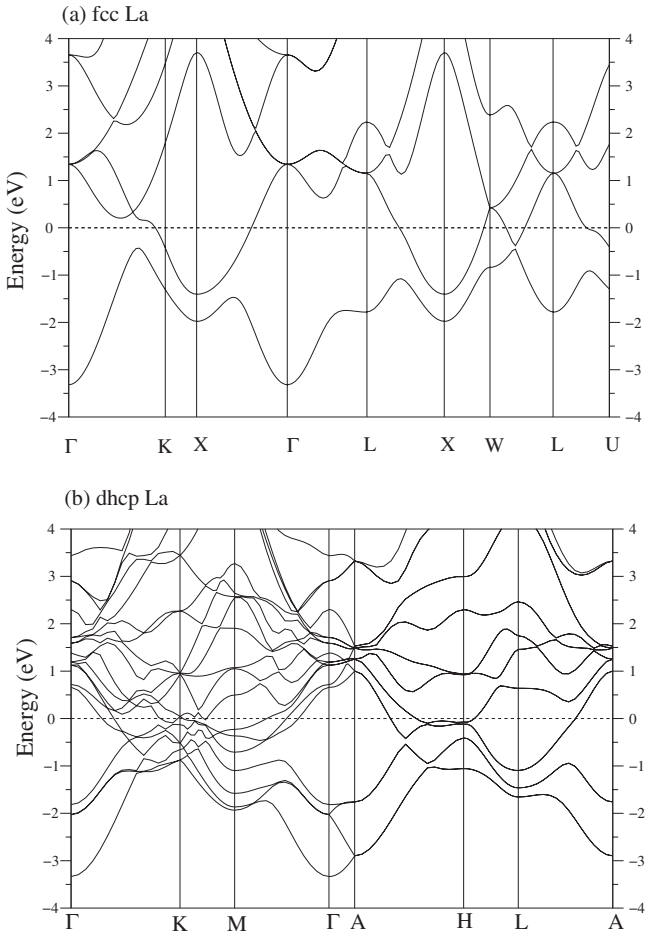

FIG. 2. The electronic structures of the fcc and dhcp phases of lanthanum.

III. RESULTS

A. Structural properties

We have used the cubic symmetry with point-group O_h and space group $Fm\bar{3}m$ for the fcc La, which is shown in Fig. 1(a). This structure is very simple and includes only one atom at (0,0,0). On the other hand, the hexagonal symmetry with point-group D_{6h} and space group P_{6_3}/mmc was invoked in our calculations for the dhcp La [see Fig. 1(b)]. This structure is different from the well known hexagonal-close-packed (hcp) structure, in that the stacking sequence is ABAC for dhcp instead of ABAB for hcp. This results in doubling of the c-axis lattice constant and thus an ideal c/a ratio of $2\times\sqrt{8/3}=3.2650$. This structure includes four atoms per unit cell, with the atomic positions in the lattice coordinates as (0,0,0), (0,0,1/2), (1/3,2/3,1/4), and (2/3,1/3,3/4). For the calculation of the bulk static properties in the fcc phase, we evaluated the total energy as a function of lattice constant. In order to obtain the equilibrium lattice parameters (a and c) for dhcp La, energy minimization has been made by following a two step procedure. For a given unit cell volume $V=\frac{\sqrt{3.0}a^2c}{2}$, total energy was minimized with respect to c/a. This step was repeated for other volumes near the experimental one. The calculated ground-state energy plotted as

TABLE I. Static properties of fcc and dhcp lanthanum and their comparison with previous experimental and theoretical results.

Source	a(Å)	C(Å)	B(GPa)	B'
fcc La	5.350		25.70	2.60
LAPW[a]	5.310			
LAPW[b]	5.320		26.10	2.78
LMTO[c]	5.110		24.00	3.00
GGA[d]	5.344		26.59	2.66
Experimental[e]	5.31		24.80	2.80
Experimental[f]			23.10	
dhcp La	3.801	12.262	26.30	2.89
LDA[g]	3.619	11.678	30.00	
GGA[h]			27.50	
GGA[g]	3.784	12.203	24.39	
Experimental[e]	3.773	12.081		
Experimental[i]			24.3	

[a]Reference 19.
[b]Reference 20.
[c]Reference 14.
[d]Reference 24.
[e]Reference 36.
[f]Reference 37.
[g]Reference 21.
[h]Reference 15.
[i]Reference 38.

function of volume for fcc and dhcp La is shown in Fig. 1(c). Finally, around the region of the total energy minimum, the bulk modulus B, the pressure coefficient B', and the equilibrium volume for fcc and dhcp La were obtained by fitting the numerical data to Murnaghan's equation state.[35] The calculated equilibrium lattice parameters (a and c), bulk modulus (B), and the pressure derivative of the bulk modulus (B'), for both structures as determined at zero pressure ($P=0$ GPa), are given in Table I. In general, there is good agreement between our results and previous experimental and theoretical results for both phases of La. In particular, the equilibrium lattice constant of fcc La is calculated to be 5.35 Å which compares well with the experimental value of 5.31 Å. Our calculated value of 25.70 GPa for bulk modulus of fcc La is only 4% larger than its experimental value of 24.80 GPa. For the dhcp phase, the computed lattice constants a and c deviate from the measured values by no more than 2.8% and 1.5%, respectively. The overestimation in the lattice parameters is a common feature with GGA calculations. The calculated bulk modulus (B) for dhcp is 26.30 GPa which is larger than its experimental value[38] of 24.3 GPa by around 8%. For dhcp La, the agreement between our and previous GGA calculations[15,21] is satisfactory, while our GGA results are slightly different from the LDA results.[21]

B. Electronic properties

The electronic band structures for fcc and dhcp La are displayed in Fig. 2. This figure clearly shows the metallic nature of both phases. There is considerable amount of overlap of bands close to the Fermi energy for dhcp La along the Γ-K and Γ-M symmetry directions while only one band

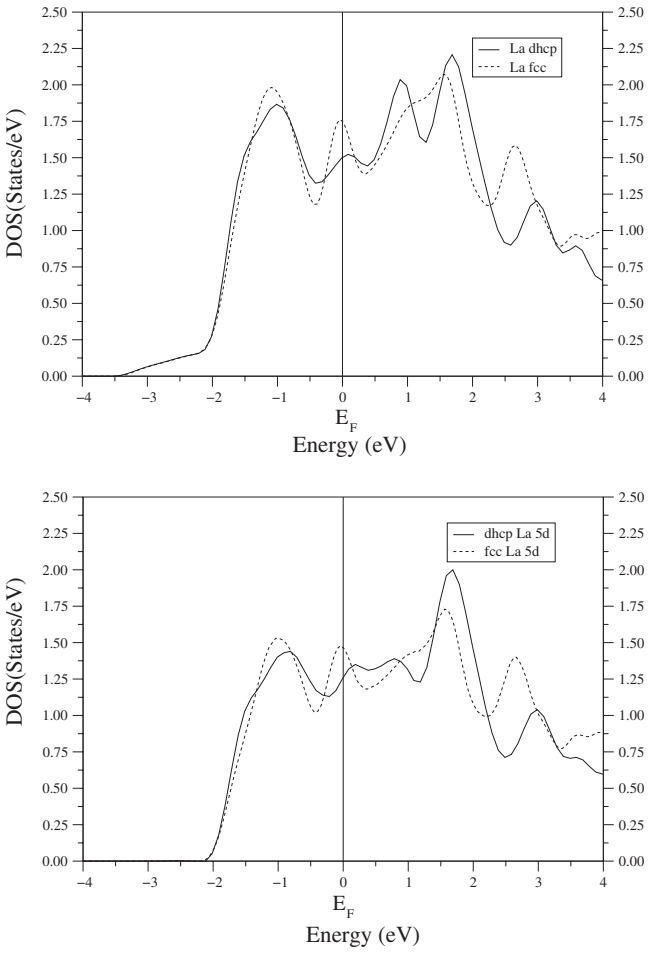

FIG. 3. Total and partial electronic density of states for fcc and dhcp La.

crosses the Fermi level for fcc La. The unoccupied and occupied bands are well separated from each other along the Γ-A and Γ-L symmetry directions for the dhcp and fcc La respectively. This similarity is expected because the Γ-A direction in the Brillouin zone of the dhcp structure maps nearly half of the Γ-L direction in the Brillouin zone of fcc structure. As expected, the states around the Fermi level for both structures are mainly of La 5d character. The overall band profiles for both phases are found to be in fairly good agreement with previous theoretical results.[16,17,21]

The calculated total and partial density of states (DOS) for fcc and dhcp La are shown in Fig. 3. All peaks between −4 and 4 eV are mainly due La 5d states for both structures, with very small contributions from La 6s and 6p states. Thus, the DOS at the Fermi level $[N(E_F)]$ is mainly due to La 5d states for both phases. The values of $N(E_F)$ are found to be 1.63 states/eV for fcc La and 1.49 for dhcp La, indicating the metallic behavior of both structures. Obviously, the 5d states give rise to electrical conductivity in both structures, though d electrons are generally considered as less efficient conductors. Our calculated $N(E_F)$ value for dhcp La being smaller than the corresponding value for fcc La has also been noted in previous theoretical calculations.[21] A comparison of the numerical values of $N(E_F)$ for fcc and dhcp La in Table II shows good agreement with previously reported theoretical results.

TABLE II. The calculated density of states at the Fermi level for fcc and dhcp La and their comparison with previous theoretical results.

	This work	LAPW GGA (Ref. 21)	LMTO LDA (Ref. 16)	LMTO LDA (Ref. 17)	RAPW LDA (Ref. 18)	RAPW LDA (Ref. 13)	LAPW LDA (Ref. 19)
$N(E_F)^{\text{fcc}}$ (states/eV)	1.63	2.21		2.27		1.82	2.02
$N(E_F)^{\text{dhcp}}$ (states/eV)	1.49	1.90	1.51	2.13	1.43		

C. Phonon spectrum

In Fig. 4, we have presented the phonon dispersion curves and the phonon density of states for La in the fcc and dhcp phases. As may be seen, all phonon frequencies for both structures are positive and there are no phonon branches with dispersions that dip toward the zero frequency. This indicates that the both phases of La are dynamically stable. In this figure, the experimental results for fcc La are shown by circles (open and filled) for $T=295$ K and by triangles (open and filled) for $T=10$ K. Unfortunately, there are no experimental data to compare our dhcp results. The agreement between our results and experimental results for fcc La is satisfactory. In particular, the agreement is excellent for the phonon branches along the [100] and [110] directions. A striking feature of the phonon spectrum is that the lower transverse acoustic (TA) acoustic branch becomes very soft along the [111] direction. Along this symmetry direction, the lower TA branch acquires a "dip" at the L point. The transi-

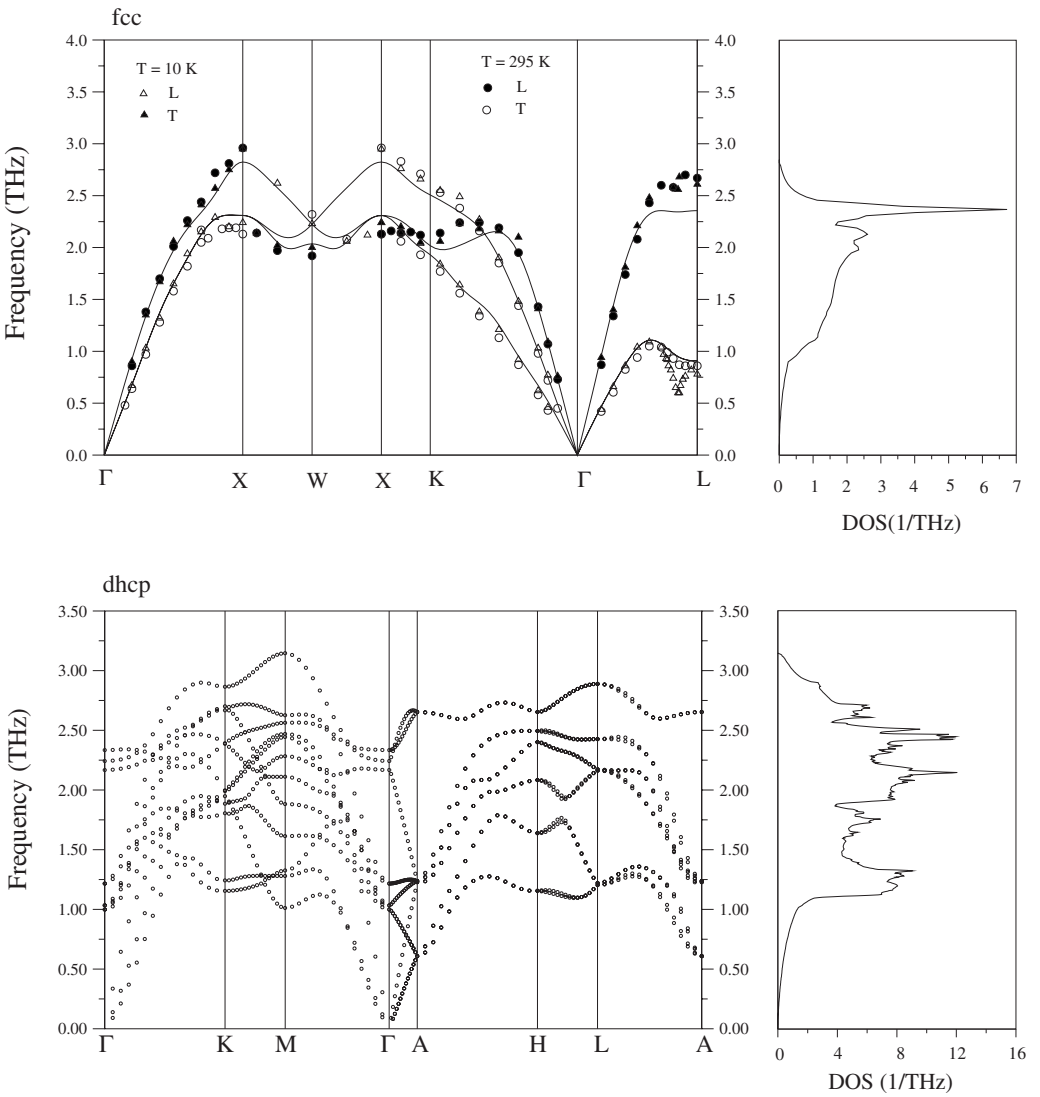

FIG. 4. Calculated phonon spectrum and vibrational density of states for fcc and dhcp La. For fcc La, open and closed circles are experimental data at $T=295$ K, while open and closed triangles indicate experimental data at $T=10$ K (Ref. 23).

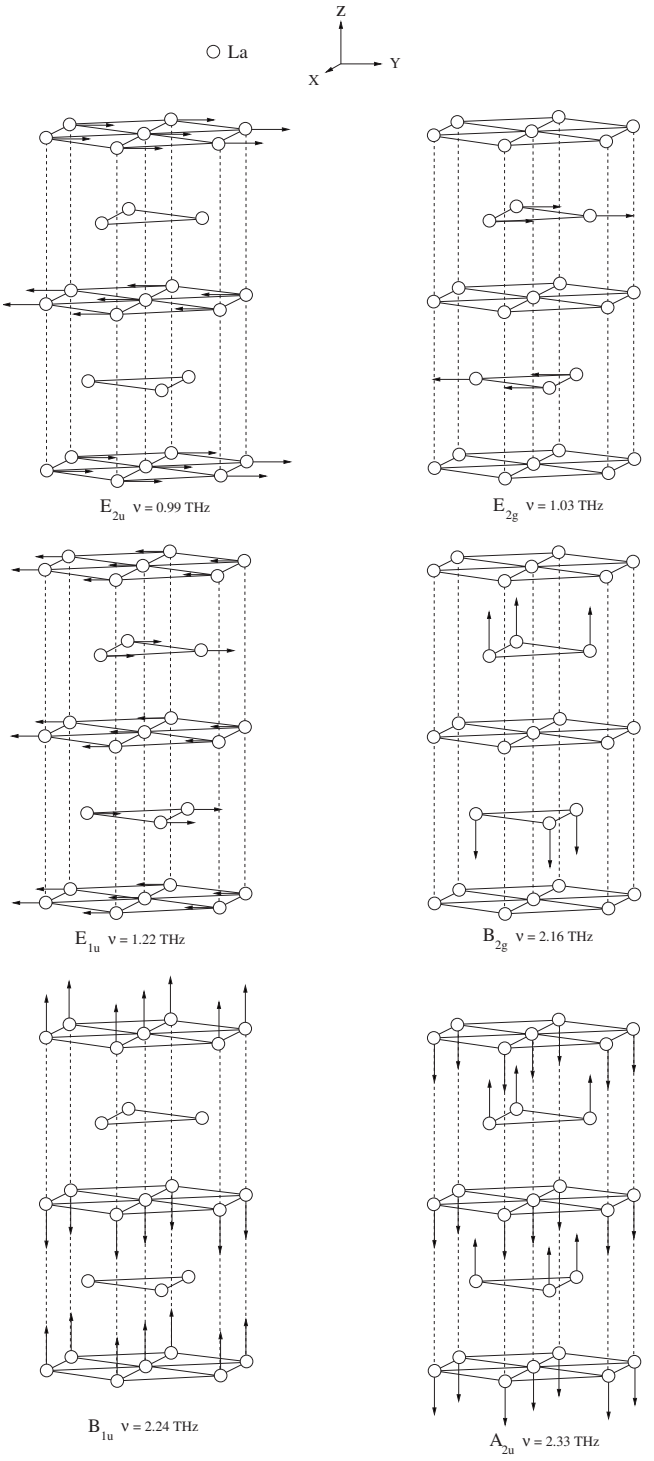

FIG. 5. Eigenvector representation of the zone-center phonon modes in double hexagonal-close-packed lanthanum.

tion to anomalous dispersion is observed at about $\mathbf{q} = \frac{2.\pi}{a}(0.31, 0.31, 0.31)$ along [111]. At this $\mathbf{q}$ point the frequency of the TA mode has the maximum frequency of 1.3 THz. In agreement with the experimental results, no anomalies occur in the longitudinal acoustic (LA) branch along any symmetry directions. It can be seen from a critical assessment of the phonon density of states for fcc La that there are four characteristic features. A sharp peak near 2.3 THz is

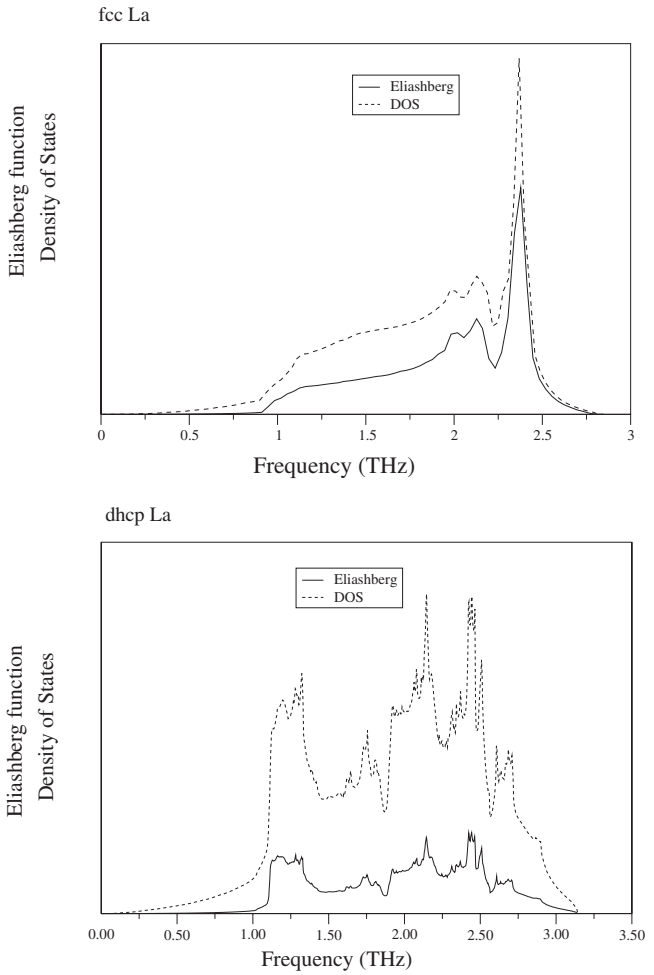

FIG. 6. A comparison of the phonon density of states (dashed lines) and Eliashberg spectral function $\alpha^2F(\omega)$ (solid lines) for both phases of lanthanum.

characterized by the LA branch. A low peak doublet feature centered around 2.1 THz is due to the TA branches in fcc La. Finally, the TA branches generate a shoulder at around 1.2 THz.

The atomic displacements in dhcp La generate the 12-dimensional irreducible representation which contains three acoustic modes and nine optical modes. These twelve branches can be seen clearly along the Γ-K direction. However, the situation is simplified along the directions where the irreducible representations have higher dimensions. Along the Γ-A (Δ line) there are only eight phonon modes: four longitudinal modes belonging to the one-dimensional representations Δ_1 and Δ_4, and four transverse modes belonging to the two-dimensional representations Δ_5^2 and Δ_6^2 ($\Delta = 2\Delta_1 + 2\Delta_4 + 2\Delta_5^2 + 2\Delta_6^2$). Moreover, at the zone boundary A, there are only four modes: two doubly degenerate longitudinal modes and two fourfold degenerate transverse modes. The computed acoustic branches behave normally in the long-wave limit with steep slopes. The interesting aspect of the phonon spectrum is the anomalous dispersion exhibited by the lower acoustic branch along the Γ-M direction close to the zone boundary M. Thus, this phonon branch exhibits a dip at the M point. Away from the zone center, all the optical

TABLE III. Calculated values of electronic parameters related to the superconducting transition in dhcp La. The calculated results are also compared with previous experimental and theoretical values.

Parameter	This work	LAPW (Ref. 21)	LMTO (Ref. 16)	EMC (Ref. 22)	Expt. (Ref. 4)	Expt. (Ref. 10)	Expt. (Ref. 11)	Expt. (Ref. 7)
λ	0.97	0.83	0.90	0.83			0.85	
T_C	4.87	4.36		5.04	4.87	5.04	5.05	4.96
η	2.09	2.30	2.37					
$\gamma_{\text{ehc}}(\frac{\text{m J}}{\text{mol K}^2})$	6.92				9.4	9.45		
$N(E_F)V_p$	0.294			0.398	0.280	0.284		
$\omega_{\ln}$ (K)	82							
$\langle\omega\rangle$ (K)	88							
$(\langle\omega^2\rangle)^{1/2}$ (K)	91							
2Δ (meV)	1.48					1.62		1.60

phonon branches are quite dispersive along all the symmetry directions. Figure 4 also shows the calculated phonon density of states for dhcp La. Several interesting features are that the frequencies of the acoustic modes are quite low (less than 1.5 THz) while optic modes are strongly dispersive with no sharp peaks as usually observed in several metals.

The zone-center phonon modes are of special theoretical interest because they can be observed by various experimental methods. The optical zone-center phonon modes in dhcp belong to the following irreducible representations: $E_{2u}+E_{2g}+E_{1u}+B_{2g}+B_{1u}+A_{2u}$. Each E vibration is twofold degenerate. Thus, we have a total of six phonon modes with nonzero frequencies. The frequencies of these six phonon modes are found to be 0.99 THz (E_{2u}), 1.03 THz (E_{2g}), 1.22 THz (E_{1u}), 2.16 THz (B_{2g}), 2.24 THz (B_{1u}), and 2.33 THz (A_{2u}). In addition to their frequencies, the eigendisplacements of these phonon modes are displayed in Fig. 5. The lowest one (E_{2u}) comes from opposing vibrations of intermediate A layer La atoms against other A layer La atoms. Atoms in the B and C layers [seen arranged in triangles in Fig. 1(b)] do not move for the E_{2u} mode. For the E_{2g} mode atoms in the B and C layers vibrate against each other while atoms in the A layer are stationary. The E_{1u} mode includes atomic vibrations from all the La atoms in the unit cell. This phonon mode is characterized by vibrations of atoms in the B and C layers in one direction and of atoms in the A layer in the opposite direction. The B_{2g} phonon mode is due to opposing vibrations of atoms in the B and C layers in the [001] direction while all A-layer atoms are stationary. For the B_{1u} phonon mode, neighboring A-layer La atoms move against other in the [001] direction. Finally, all the La atoms in the unit cell vibrate for the A_{2u} mode.

D. Electron-phonon interaction and superconductivity in dhcp La

Figure 6 presents the calculated electron-phonon spectral function $\alpha^2F(\omega)$ and the phonon density of states for fcc and dhcp La. One can see that the shape of the electron-phonon spectral function is similar to that of the phonon density of states for both phases in the entire frequency range. This observation indicates that phonons of all frequencies contribute to the electron-phonon coupling for both structures. Table III shows the calculated values of the superconducting state parameters for dhcp. In general, our results are in qualitative agreement with available experimental[4,7,10,11] and theoretical[16,21,22] results. The calculated result for the total electron-phonon interaction parameter, $\lambda=0.97$, compares well with previous theoretical[16,21,22] and experimental[11] values. The logarithmically averaged frequency ($\omega_{\ln}$) is found to be 82 K from Eq. (10). Unfortunately, we could not find any theoretical and experimental results for the logarithmically averaged frequency to compare our results with. After obtaining λ and $\omega_{\ln}$, the superconducting transition temperature (T_C) is calculated from Eq. (9). For the normal choices, $\mu^*=0.1$, 0.11, 0.12, 0.13, and 0.14, T_C is found to be 5.41, 5.14, 4.87, 4.61, and 4.35 K, respectively. All the obtained values compare very well with the corresponding experimental values of 4.87,[4] 4.96,[7] 5.04,[10] and 5.05 K.[11] Our calculated electronic stiffness constant ($\eta=2.09$) is slightly lower than the previously reported theoretical values of 2.30 (LAPW) (Ref. 21) and 2.37 (LMTO).[16] The electronic stiffness constant can be written as $\eta=N(E_F)\langle I^2\rangle$. Where $\langle I^2\rangle$ is the mean-square electron-ion matrix element. As can seen from Table II, our calculated $N(E_F)$ value is smaller than the corresponding LAPW (Ref. 21) and LMTO (Ref. 16) values. As a result of

TABLE IV. Comparison of superconducting state parameters for dhcp La and fcc La. The parameter μ^* is taken to be 0.12.

Phase	λ	T_C	η	$N(E_F)V_p$	$\omega_{\ln}$ (K)	$\langle\omega\rangle$ (K)	$(\langle\omega^2\rangle)^{1/2}$ (K)	2Δ (meV)
fcc	1.06	5.88	2.30	0.308	85	92	93	1.79
dhcp	0.97	4.87	2.09	0.294	82	88	91	1.48

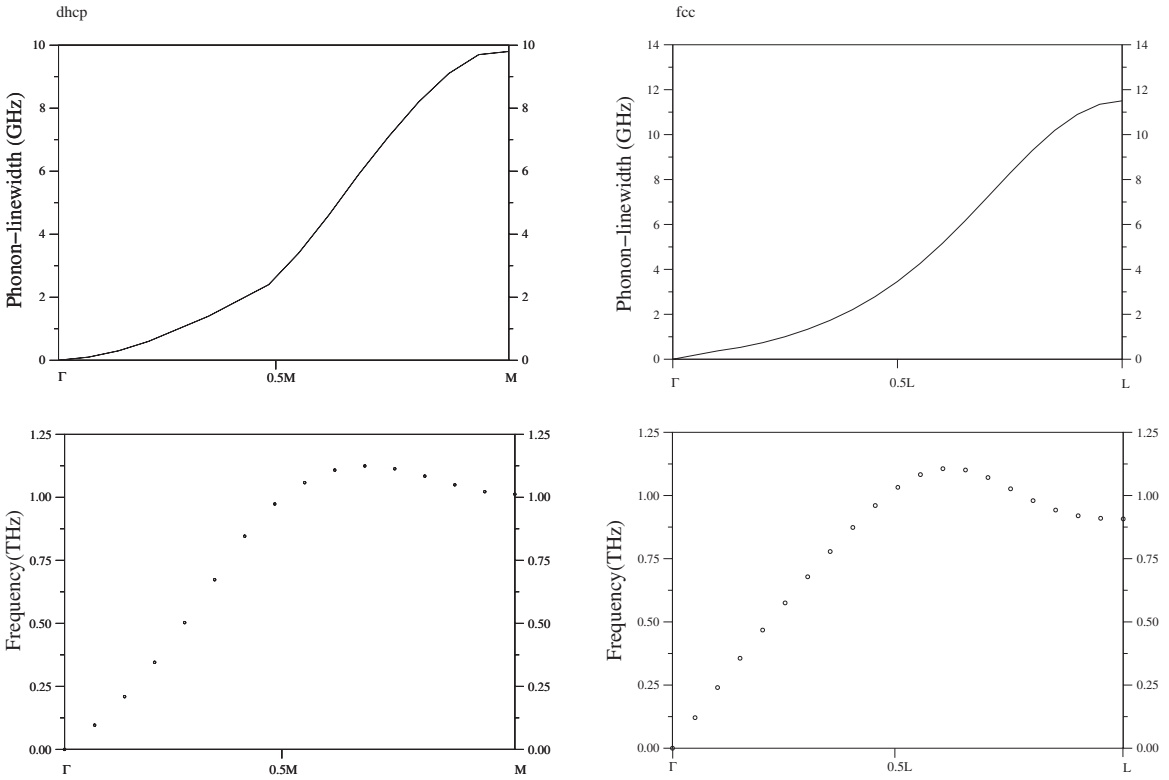

FIG. 7. Phonon linewidth ($\gamma_{\mathbf{q}j}$) and phonon frequency dispersion for the lower acoustic phonon branch in dhcp La (fcc La) along the Γ-*M* (the Γ-*L*) symmetry direction.

this difference, we get a smaller value for the η constant than the other theoretical calculations.[16,21] In our *ab initio* calculations, $N(E_F)V_p$ is found to be 0.294, which compares very well with the experimental values of 0.280 (Ref. 4) and 0.284.[10] Finally, the superconducting energy gap $2\Delta = 1.48$ eV is nearly 0.1 eV lower than its experimental value of 1.60 eV.[7] Table IV presents a comparison of the superconducting parameters for dhcp La and fcc La in Table IV. One can see that the values of superconducting parameters for dhcp La are all lower than their corresponding values for fcc La. This can be related to the difference between the calculated $N(E_F)$ values of both phases. The calculated $N(E_F)$ value of 1.49 states/eV for dhcp La is smaller than the corresponding value of 1.63 states/eV for fcc La, which can be seen in Fig. 3 clearly. This causes a smaller Hopfield parameter ($\eta = N(E_F)\langle I^2\rangle$) and a smaller electron-phonon coupling constant [see Eq. (6)] for dhcp La. Thus, the superconducting transition temperature for dhcp La is lower than that for fcc La.

In order to establish a correlation between the anomalous phonon dispersion and the electron-phonon interaction, we have calculated the phonon linewidth $\gamma_{\mathbf{q}j}$ for the lower transverse acoustic phonon branch in both structures (see Fig. 7). As we have mentioned before, the TA branch in fcc La has a dip with the value of 0.90 THz at the *L* point. However, the phonon linewidth $\gamma_{\mathbf{q}j}$ of lower TA branch reaches the largest value, indicating much larger electron-phonon interaction at the *L* point. At this **q** point, the electron phonon coupling parameter is found to be largest with the value of 1.32. This result clearly indicates the correlation between phonon

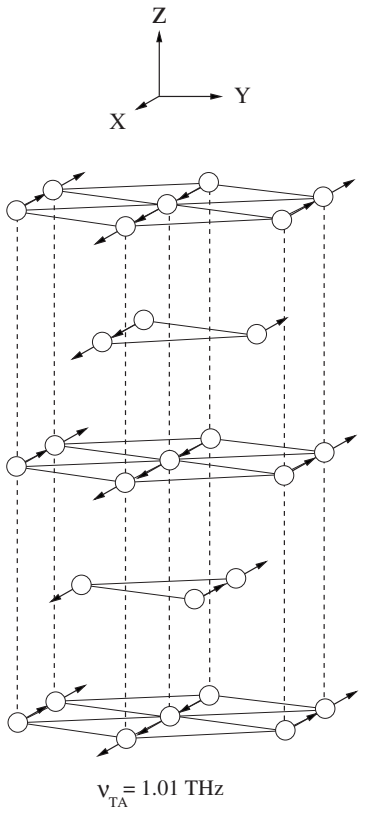

FIG. 8. Eigenvector representation of the lower transverse acoustic (TA) phonon mode at the *M* point in the Brillouin zone for the double hexagonal-close-packed lanthanum.

anomalies and superconductivity. Although the lowest acoustic branch of dhcp La shows a dip at the M point on the zone boundary, we have not observed a dip for the phonon linewidth at this symmetry point. This is a result of large electron-phonon interaction for this phonon branch at the M point. This is a second sign for the correlation between phonon anomalies and superconductivity. At this **q** point, the electron-phonon coupling parameter for the lowest acoustic phonon mode is found to be $\lambda_M^{\mathrm{TA}}=0.30$. The frequency of this phonon mode is 1.01 THz. A schematic representation of atomic vibrations for this phonon mode is displayed in Fig. 8. It clearly shows that the vibrational amplitudes of La atoms along [100] may cause their d orbitals to overlap, leading to strong electron-phonon coupling of this phonon mode at the M point.

IV. SUMMARY

In this work, we have presented a theoretical analysis of the structural and electronic properties of the face-centered-cubic and double hexagonal-close-packed lanthanum by using the generalized gradient approximation of the density functional theory and the plane wave *ab initio* pseudopotential method. The equilibrium lattice parameters, bulk modulus and its pressure derivative for both phases are in good agreement with previous theoretical and experimental findings. Our calculated electronic structure agrees well with previous theoretical electronic structures, and clearly indicates the metallic character of these structures. The main contribution to the density of states at the Fermi level comes from the $5d$ states of La. The phonon spectrum and density of states for both phases do not show any unstable mode, confirming that these structures are dynamically stable. The polarizations of zone-center phonon modes for dhcp La are discussed in detail. A striking feature in the phonon spectrum of dhcp is the softening of the lowest acoustic branch along the Γ-M direction while a similar feature has been observed along the Γ-L direction for fcc La. The total electron-phonon coupling parameter is found to be 0.97 for dhcp La and 1.06 for fcc La. Using these values, several parameters related to the superconducting transition such as T_C, η, $N(E_F)V_p$, $\omega_{\ln}$, $\langle\omega\rangle$, $(\langle\omega^2\rangle)^{1/2}$, and 2Δ are calculated and compared with previous experimental and theoretical results. In particular, our calculated T_C values of 4.87 K (dhcp La) and 5.88 K (fcc La) are in excellent agreement with the experimental results of around 5 K (dhcp La) and 6 K (fcc La). A comparison of the superconducting parameters for dhcp La and fcc La shows that the values are lower for the dhcp phase. This is related to the lower electronic density of states at the Fermi level for the dhcp phase.

[1] K. A. Gschneidner, Jr., Solid State Phys. **16**, 275 (1964).
[2] D. K. Finnemore, D. L. Johson, J. E. Ostenson, F. H. Spedding, and B. J. Beaudry, Phys. Rev. **137**, A550 (1965).
[3] F. Smith and W. E. Gardner, Phys. Rev. **146**, 291 (1966).
[4] D. L. Johnson and D. K. Finnemore, Phys. Rev. **158**, 376 (1967).
[5] J. S. Rogers and S. M. Khana, Phys. Rev. Lett. **20**, 1284 (1968).
[6] M. B. Maple, J. Witting, and K. S. Kim, Phys. Rev. Lett. **23**, 1375 (1969).
[7] L. F. Lou and W. J. Tomasch, Phys. Rev. Lett. **29**, 858 (1972).
[8] H. Wühl, A. Eichler, and J. Wittig, Phys. Rev. Lett. **31**, 1393 (1973).
[9] H. Balster and J. Witting, J. Low Temp. Phys. **21**, 377 (1975).
[10] P. H. Pan, D. K. Finnemore, A. J. Bevolo, H. R. Shanks, B. J. Beaudry, F. A. Schmidt, and G. C. Danielson, Phys. Rev. B **21**, 2809 (1980).
[11] Ö. Rapp and B. Sundqvist, Phys. Rev. B **24**, 144 (1981).
[12] V. G. Tissen, E. G. Ponyatovskii, M. V. Nefedova, F. Porsch, and W. B. Holzapfel, Phys. Rev. B **53**, 8238 (1996).
[13] H. M. Myron and S. H. Liu, Phys. Rev. B **1**, 2414 (1970).
[14] T. Takeda, J. Kbler, J. Phys. F: Met. Phys. **9**, 661 (1979).
[15] A. Delin, L. Fast, B. Johansson, O. Eriksson, and J. M. Wills, Phys. Rev. B **58**, 4345 (1998).
[16] H. L. Skriver and I. Mertig, Phys. Rev. B **41**, 6553 (1990).
[17] T. Jarlborg, G. Andersson, B. Sundqvist, and O. Rapp, J. Phys.: Condens. Matter **1**, 8407 (1989).
[18] G. S. Fleming, S. H. Liu, and T. L. Loucks, J. Appl. Phys. **40**, 1285 (1969).
[19] C. W. Pickett, A. J. Freeman, and D. D. Koelling, Phys. Rev. B **22**, 2695 (1980).
[20] Z. W. Lu, D. J. Singh, and H. Krakauer, Phys. Rev. B **39**, 4921 (1989).
[21] L. W. Nixon, D. A. Papaconstantopoulos, and M. J. Mehl, Phys. Rev. B **78**, 214510 (2008).
[22] A. M. Vora, Cent. Eur. J. Phys. **6**, 263 (2008).
[23] C. Stassis, C.-K. Loong, and J. Zarestky, Phys. Rev. B **26**, 5426 (1982).
[24] G. Y. Gao, Y. L. Niu, T. Cui, J. Zhang, Y. Li, Y. Xie, Z. He, Y. M. Ma and G. T. Zou, J. Phys.: Condens. Matter **19**, 425234 (2007).
[25] H. M. Tütüncü and G. P. Srivastava, J. Appl. Phys. **104**, 063916 (2008).
[26] S. Baroni, S. de Gironcoli, A. Dal Corso, and P. Giannozzi, Rev. Mod. Phys. **73**, 515 (2001) http://www.pwscf.org.
[27] W. Kohn and L. J. Sham, Phys. Rev. **140**, A1133 (1965).
[28] D. Vanderbilt, Phys. Rev. B **41**, 7892 (1990).
[29] J. P. Perdew, K. Burke, and M. Ernzerhof, Phys. Rev. Lett. **77**, 3865 (1996).
[30] H. J. Monkhorst and J. D. Pack, Phys. Rev. B **13**, 5188 (1976).
[31] S. Baroni, P. Giannozzi, and A. Testa, Phys. Rev. Lett. **58**, 1861 (1987).
[32] W. L. McMillan, Phys. Rev. **167**, 331 (1968).
[33] P. B. Allen, Phys. Rev. B **6**, 2577 (1972).
[34] P. B. Allen and R. C. Dynes, Phys. Rev. B **12**, 905 (1975).
[35] F. D. Murnaghan, Proc. Natl. Acad. Sci. U.S.A. **50**, 697 (1944).
[36] K. Syassen and W. B. Holzapfel, Solid State Commun. **16**, 533 (1975).
[37] N. Singh and S. P. Singh, Phys. Rev. B **42**, 1652 (1990).
[38] C. Kittel, *Introduction to Solid State Physics*, 7th ed. (Wiley, New York, 1996).